Electrical conduction of Ge nanodot arrays formed on an oxidized Si surface

Yasuo Nakayama[a)]
Core Research for Evolutional Science and Technology (CREST), Japan Science and Technology Agency (JST), Saitama 332-0012, Japan

Shiro Yamazaki, Hiroyuki Okino, Toru Hirahara,[b)] Iwao Matsuda,[b)] and Shuji Hasegawa[b)]
Department of Physics, Graduate School of Science, The University of Tokyo, 7-3-1 Hongo, Bunkyo-ku, Tokyo 113-0033, Japan

Masakazu Ichikawa[b)]
Quantum-Phase Electronics Center, Department of Applied Physics, Graduate School of Engineering, The University of Tokyo, 7-3-1 Hongo, Bunkyo-ku, Tokyo 113-8656, Japan

(Received 14 May 2007; accepted 22 August 2007; published online 18 September 2007)

Carrier transport mechanism on Ge nanodot arrays formed on SiO_2 monolayer covering over the Si surface is investigated by microscopic four-point-probe measurements combined with core-level photoemission spectroscopy and scanning tunneling microscopy. Different conduction natures are found depending on whether or not the nanodots and the substrate are directly connected by subnanometer-sized voids penetrating the SiO_2 layer. In the presence of the voids, conductivity is regulated by the dot-size through quantum-size effect. © *2007 American Institute of Physics*. [DOI: 10.1063/1.2784181]

Spherical Ge nanodots self-organized on a Si surface covered with an ultrathin (~0.3 nm) SiO_2 layer are particularly promising from a point of view of Si-based optoelectronics application owing to the occurrence of quantum size effect,[1–3] extremely high density ($>10^{12}$ cm^{-2}),[4] and photoluminescence capability.[5,6] Under appropriate conditions, a part of SiO_2 is destroyed by a reaction with deposited Ge resulting in formation of voids which penetrate the SiO_2 monolayer by diameter of less than 1 nm. The voids function as nucleation centers, and further deposition generates Ge nanodots connecting directly to the Si substrate through the voids. Such nanodots are epitaxial to the Si substrate, which provides a reflection high energy electron diffraction (RHEED) pattern with transmission spots of epitaxial Ge dots [Fig. 1(a), left]. On the other hand, high deposition rate gives nonepitaxial nanodots separated from the substrate by the SiO_2 monolayer because the nucleation becomes faster than the void-formation, which provides another RHEED pattern with Debye rings [Fig. 1(a), right].

Recently, we revealed that the epitaxial nanodots have lower potential barrier (2.1 eV) for confining carriers therein than the nonepitaxials (6.7 eV).[1] Such a reduced barrier can, however, substantially confine the carriers into the epitaxial nanodots even though the voids connect the dots to the substrate. Variation in the confining potential barrier is expected to affect the carrier exchange at the dot-substrate interface that is a requisite information to apply these nanodots to optoelectronics devices. Actually, different transport natures were reported at the interface for two types of Ge dots formed on Si(100), which are ascribed to the different interface conditions with/without a barrier.[8] In the present study, we have demonstrated four-point-probe conductivity measurements in micrometer scale combined with core-level photoemission spectroscopy (PES) and scanning tunneling microscopy (STM) for the sake of clarifying how the carriers behave depending on the interface structures with different potential barriers.

Preparation of the SiO_2 monolayer and estimation of Ge deposition rate were conducted by the same procedures as

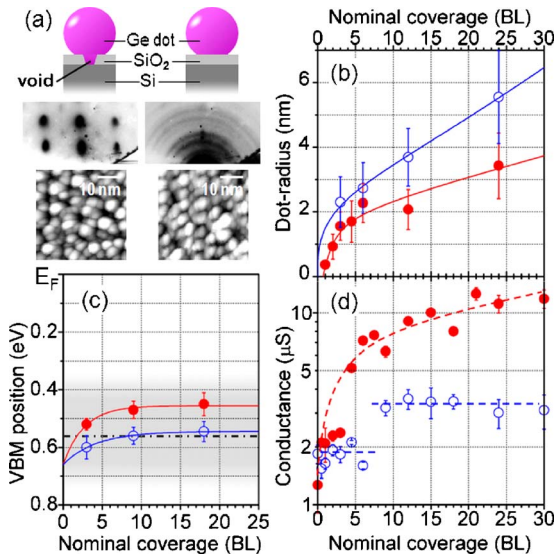

FIG. 1. (Color online) (a) Schematic drawings, typical RHEED patterns, and STM images of epitaxial (left) and nonepitaxial (right) Ge nanodots. For STM images, r is the same (~2.5nm) for the two types of nanodots. (b) The average dot-radius r estimated by a statistical analysis of the STM images, (c) the VBM position of Si from E_F evaluated from Si-2p energy shift, and (d) electrical conductance obtained from the gradient at zero current of I-V curves taken at 320 K, plotted as a function of nominal Ge coverage. Solid lines indicate fitting curves, whereas dashed lines are guides for eyes. Error bars show standard deviation of size distribution of the nanodots. Filled and open symbols correspond to the epitaxial and nonepitaxial dots, respectively. The VBM position when E_F states at the center of the band gap is shown in a dash-dotted line in (c), and a gray-hatched area corresponds to depletion and week-inversion region.

[a)]Present address: Center for Frontier Science, Chiba University, 1-33 Yayoi, Inage-ku, Chiba 263-8522, Japan. Electronic mail: nkym@restaff.chiba-u.jp
[b)]Also at CREST, JST, Saitama 332-0012, Japan.

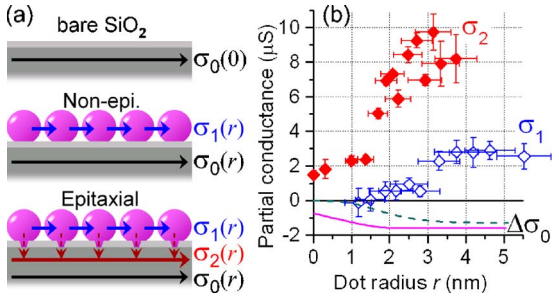

FIG. 2. (Color online) (a) Schematic drawings displaying the conduction paths contributing to the measured conductance for the bare SiO_2–Si substrate and the two types of nanodot arrays on it. (b) Conductance of each path, σ_1 and σ_2, plotted as a function of the average dot radius r. Dot-size dependent change in σ_0 from that of the bare SiO_2–Si substrate induced by shift of the VBM of Si (i.e., band-bending change) is also shown as solid and dashed lines for the epitaxial and nonepitaxial cases, respectively.

reported before.[1,3,4] The epitaxial and nonepitaxial Ge nanodots were formed on the SiO_2 monolayer kept at 550 °C at the deposition rate of $\frac{3}{4}$ and 2 BL/min (bilayers per minute), respectively, and they were distinguished from each other by RHEED patterns. Electrical conductance was evaluated from gradients of current-voltage curves around the zero point, which were measured by a monolithic four-point-probe[9] with a probe spacing of 20 μm without any perceptible damages on the surface by the probes.[10] STM observation was performed in the same condition as reported before.[1] Change in band-bending [i.e., change of energy position of the valence band maximum (VBM) with respect to the Fermi level (E_F)] of the Si substrate induced by Ge dot formation was evaluated from Si-2p PES spectra.[11] The spectra were obtained on vacuum-ultraviolet beamlines BL-1C and BL-18A at Photon Factory (PF) in High Energy Accelerator Research Organization (KEK), Japan.

In order to compare the electrical conductivities of the two types of nanodot arrays in equivalent conditions, the nominal coverage should be transformed into the dot size for the epitaxial and nonepitaxial dots. Coverage dependent variations of the average radius r of the both types of nanodots [Fig. 1(b)] are excellently fitted by an appropriate function considering both variation of the dot density and consumption of deposited Ge atoms by the void-formation reaction,[12] which allows us to convert the coverage into the corresponding dot radius (r). It also indicates that, for the epitaxial case, observable dots are not formed ($r=0$) at small coverage (e.g., 0.5 BL), which is consistent with the previous report.[4]

Si-2p peak shifts 0.03 eV to higher binding energy side after oxidation with respect to that of a clean 7×7 surface, whereas Ge deposition on the oxide layer makes the peaks move to lower binding energy. These shifts correspond to change in the VBM position of Si against that of the 7×7 [0.63 eV from E_F (Ref. 11)], as shown in Fig. 1(c). The present change will suppress the conductivity through the surface space-charge (SC) layer of Si which can be calculated by solving Poisson's equation. However, the measured conductance shows, especially for the epitaxial case, significant enhancement after the nanodot formation, as shown in Fig. 1(d). It indicates that the nanodots supply additional conduction paths onto the present system.

We simply deconvolute the measured "total" conductance into three types of paths, as sketched in Fig. 2(a); a path ascribed to lateral conduction across the nanodot arrays σ_1, a path induced by the voids on the interface oxide layer σ_2, and a path through the substrate σ_0. In other words, the total conductance of each type of nanodot arrays, which varies depending on r, can be expressed with the "partial" conductances of respective paths in parallel as,

$$\sigma^{\mathrm{NE}}(r) = \sigma_0^{\mathrm{NE}}(r) + \sigma_1(r),$$

$$\sigma^{\mathrm{epi}}(r) = \sigma_0^{\mathrm{epi}}(r) + \sigma_1(r) + \sigma_2(r),$$

where the superscripts epi and NE indicate the epitaxial and nonepitaxial dots, respectively. We can evaluate $\sigma_1(r)$ directly from the measured conductances of the nonepitaxial dots $\sigma^{\mathrm{NE}}(r)$ by subtracting $\sigma_0^{\mathrm{NE}}(r)$ calculated from the VBM shift. When r is the same, the surface morphology seems to be equivalent for the epitaxial and nonepitaxial ones as shown in Fig. 1(a). Thus, $\sigma_1(r)$ is considered to be common for the two types of nanodot arrays, which allows us to obtain $\sigma_2(r)$ from a comparison between $\sigma^{\mathrm{NE}}(r)$ and $\sigma^{\mathrm{epi}}(r)$. Figure 2(b) shows $\sigma_1(r)$ and $\sigma_2(r)$ plotted together with each $\Delta\sigma_0(r)[\equiv\sigma_0(r)-\sigma_0(0)]$. Concerning σ_1, we can find a discontinuous increase around $r=3$ nm. Such behavior can be ascribed to the formation of a percolated network of tunneling transport across the dot arrays. On the other hand, σ_2 makes dominant contribution on σ^{epi}, which implies significant effect of the voids on carrier transport.

Next, we measured temperature dependent variation of conductance. If the conduction process is dominated by thermal activation of the carriers, the activation energy (E_a) of the carriers can be evaluated from a gradient of the $(1/T)$-ln σ plot because the conductance can be approximated as the following relation: $\sigma\propto\exp(-E_a/2k_BT)$. A logarithm of conductance at each-sized dots is plotted to inverse temperature $1/T$ in Figs. 3(a) and 3(b). Concerning the epitaxial nanodot arrays, ln σ seems to be linear to $1/T$ and E_a seems to become smaller steadily when the dot size becomes larger, as shown in Fig. 3(c) (plotted as filled symbols). In contrast, for the nonepitaxial case [Figs. 3(b) and 3(d)], $r-E_a$ dependence shows different behaviors to the epitaxial case. This result also indicates that the dominant conduction process of the nonepitaxial dot arrays is diverse from that of the epitaxial ones.

For thermal activation scheme, E_a should correspond to an energy difference between occupied and unoccupied states. On the other hand, quantum size effect expands the energy gap of the Ge nanodots wider when the dot size becomes smaller.[1–3] Since the size of the nanodots will not affect the gap width of the Si substrate, the dot size dependent change of E_a observed on the epitaxial nanodot arrays is ascribed to shifting of the quantized energy levels in the Ge nanodots. However, the nanodot layer itself hardly contributes to the conductivity especially when $r<3$ nm, as shown in Fig. 2 (σ_1). It strongly suggests that most of the generated carriers on the nanodot states transport through the Si substrate.

The above discussion points out that the expected activation energy of the carrier generation is considered to be the smaller value of the following excitation energies; from the highest-occupied-state (HOS) of the Ge nanodots to conduction-band minimum (CBM) of the Si substrate and from VBM of the Si to the lowest-unoccupied state (LUS) of the Ge. These excitation energies can be calculated as a func-

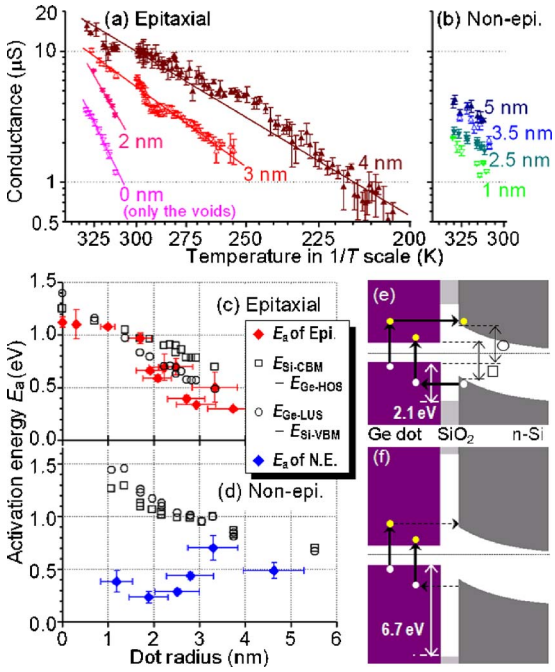

FIG. 3. (Color online) [(a) and (b)] Temperature dependence of the conductance of the two types of nanodot arrays at noted average dot radii r. [(c) and (d)] The activation energy E_a evaluated from the above $\ln \sigma - (1/T)$ relationship (filled diamonds with error bars) plotted as a function of r. Expected activation energies corresponding to overexcited electrons and holes are also shown as open squares and circles, respectively. Schematic drawings of the energy diagrams at the Ge–SiO_2–Si interfaces for the (e) epitaxial and (f) nonepitaxial nanodots.

tion of r from the energy positions of the respective band edges, as shown in Figs. 3(c) and 3(d) (open symbols). For this calculation, energy positions of the CBM of the Si substrate at the interface are determined from the VBM position, as shown in Fig. 1(c). The HOS of the Ge nanodots is estimated from our PES results reported previously,[1] and the LUS of the Ge nanodots is assumed to be symmetric to the HOS with respect to E_F.[3] In the case of the epitaxial dots, E_a evaluated from the experimental $(1/T)$-$\ln \sigma$ plots shows good agreement with the expected energy difference, as shown in Fig. 3(c). It strongly suggests that *overexcited* carriers in the Ge nanodots which can exceed the band offsets between Ge and Si dominate the conductivity for the epitaxial case. We therefore propose a conduction mechanism of the epitaxial dot arrays, as shown in Fig. 3(e); electrons (holes) which make a dominant contribution on the conductivity are thermally excited in the nanodots and provided for the Si substrate by tunneling through the interface barrier. On the contrary, for the nonepitaxial case, the *apparent* E_a is irrelevant to the expected energy difference, which strongly suggests that such overexcited carriers play a trivial role on the conduction process. Since the expected energy difference is equivalent for the both types of nanodots, the diversity of the conduction mechanism should be ascribed to the tunneling process at the interface SiO_2 monolayer. Carrier provision from the nanodots to the substrate is diminished by the large potential barrier for the nonepitaxial dots; whereas the reduced potential barrier, owing to the voids, enables the epitaxial dots to supply the carriers enhancing conductivity to the substrate.

In conclusion, electrical conductivity of the epitaxial and nonepitaxial nanodot arrays formed on the oxidized Si substrate was systematically investigated as a function of dot size with a microscopic four-point-probe method. Concerning the nonepitaxial case, the dot array and the substrate are considered to be electrically separated from each other by the SiO_2 monolayer. The subnanometer-sized voids interconnecting the nanodots and the substrate enable the epitaxial dots to supply the carriers to the substrate, which leads significant conductance gain for the epitaxial dot arrays.

The authors would like to thank Professor A. Kakizaki and Ms. A. Harasawa of ISSP and Professor K. Ono of KEK for their help during the PES experiments at PF. A part of this work was performed under the approval of the PF Program Advisory Committee (Proposal No. 2005G089). This work was financially supported by CREST, JST, and by the Japanese Society for the Promotion of Science (JSPS).

[1] Y. Nakayama, I. Matsuda, S. Hasewaga, and M. Ichikawa, Appl. Phys. Lett. **88**, 253102 (2006).
[2] A. Konchenko, Y. Nakayama, I. Matsuda, S. Hasegawa, Y. Nakamura, and M. Ichikawa, Phys. Rev. B **73**, 113311 (2006).
[3] Y. Nakamura, K. Watanabe, Y. Fukuzawa, and M. Ichikawa, Appl. Phys. Lett. **87**, 133119 (2005).
[4] A. A. Shklyaev, M. Shibata, and M. Ichikawa, Phys. Rev. B **62**, 1540 (2000).
[5] A. A. Shklyaev and M. Ichikawa, Appl. Phys. Lett. **80**, 1432 (2002).
[6] A. A. Shklyaev, S. Nobuki, S. Uchida, Y. Nakamura, and M. Ichikawa, Appl. Phys. Lett. **88**, 121919 (2006).
[7] Y. Nakamura, Y. Nagadomi, K. Sugie, N. Miyata, and M. Ichikawa, J. Appl. Phys. **95**, 5014 (2004).
[8] H.-C. Chung, W.-H. Chu, and C.-P. Liu, Appl. Phys. Lett. **89**, 082105 (2006).
[9] T. Tanikawa, I. Matsuda, R. Hobara, and S. Hasegawa, e-J. Surf. Sci. Nanotechnol. **1**, 50 (2003).
[10] I. Shiraki, T. Nagao, S. Hasegawa, C. L. Petersen, P. Bøggild, T. M. Hansen, and F. Grey, Surf. Rev. Lett. **7**, 533 (2000).
[11] F. J. Himpsel, G. Hollinger, and R. A. Pollak, Phys. Rev. B **28**, 7014 (1983).
[12] Y. Nakayama, I. Matsuda, S. Hasewaga, and M. Ichikawa (unpublished).